The Physics of Cell Membranes

Article *in* Journal of Biological Physics · December 2003

DOI: 10.1023/A:1027362704125 · Source: PubMed

1 author:

Hans Gerard Leonard Coster
The University of Sydney
205 PUBLICATIONS **4,834** CITATIONS

Journal of Biological Physics **29:** 363–399, 2003.

The Physics of Cell Membranes

H.G.L. COSTER
Department of Biophysics, School of Physics and the Centre for Membrane Science and Technology, University of New South Wales, Sydney 2051, Australia

Contents

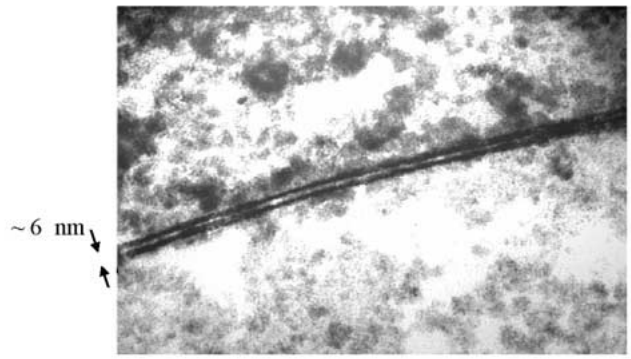

Figure 1. An electron micrograph of the plasma membrane (of *Chara corallina* (cropped from [1]). To fix the membrane for electronmicroscopy the material was crosslinked using OsO_4 which also enhances the contrast in the electron-microscope image. The two dark regions in the OsO_4 stained structure corresponds to the polar regions of the membrane and the central light region corresponds to the non-polar, hydrophobic, region.

Abstract: An overview is given of the fundamental physics underlying the self-assembly, molecular organisation and electrical properties of the membranes that envelop living cells. These ultra thin (∼6 nm) membranes act as a diffusion barrier between the cell interior (cytoplasm) and the external medium. They consist basically of a bi-molecular film of lipid molecules in which are embedded functional proteins that perform a variety of functions, including energy transduction, signalling, transport of ions (and other molecules), etc. Some examples are also presented of the fascinating and socially and commercially important applications of membrane biophysics.

Introduction and Historical Background

Introduction and historical background The plasma membranes enveloping living cells separate the exterior environment from the cytoplasm. It provides a selective diffusion barrier to molecules moving into, and out of, the cell and it contains energy driven transport mechanisms that maintain concentration differences of many substances between the external environment and the cytoplasm. Voltage-gated ion channels in the plasma membrane generate 'action' potentials in neurones that are transmitted along the membrane of nerve axons. Cells sense the presence of specific molecules in the surrounding medium when these molecules bind to specific receptor molecules embedded in the membrane and this forms the basis of the immune signalling and response system. Almost all of the biochemical processes in a cell are associated with membrane bound enzymes and transport and transduction mechanisms. An example of an electron micrograph of a plasma membrane is shown in Figure 1 (cropped from [1]).

The cell membrane is some two orders of magnitude smaller than the resolution of optical microscopes. The presence of a membrane was initially inferred from the rate of permeation of various substances into cells. Before the turn of the 19th

century, it was observed that the rates of intracellular accumulation of substances were proportional to their solubility in lipids (eg. Overton [2]). Later (1935) Danielli and Davson [3] put forward a model of the cell membrane in which a lipoidal layer is sandwiched between two proteinaceous layers. This was consistent with an earlier measurement by Gorter and Grendel [4] in 1925 who had spread the lipids extracted from red blood cells as a monolayer and determined that the area occupied by the lipids was equal to twice the total surface areas of the erythrocytes. In that same year Fricke and Morse [5] had estimated the thickness of the cell membrane from measurements of the electrical impedance of a suspension of cells. Their estimate of 20–30 nm was only a factor of $\sim$3 too large. The first direct measurement of the thickness obtained from electron-micrographs by Robertson [6] were not made until 1959. It showed that the lipoidal layer was probably only as thick as two molecules of common biological lipids. He introduced the idea of the 'unit membrane'. This concept of the presence of a bimolecular layer of lipids in cell membranes was further strengthened when in 1962 Mueller, Rudin, Tien and Wescott [7] produced the first artificial, planar, lipid bilayer membrane from lipids extracted from bovine brain.

We now know that the cell membrane consists of a bimolecular layer of lipid molecules in which are imbedded various functional proteins (e.g., see [8–11]). The bimolecular lipid membrane, or lipid bilayer, provides a fluid matrix in which the membrane proteins assume specific orientations and form functional aggregates.

The account of the physics of cell membranes below follows a logical, retrospective rather than historical order.

PART 1: THE BI-MOLECULAR LIPID MEMBRANE

1.1 Interfacial-Free Energy

At the interface between two liquid phases such as oil and water and imbalance between the (van der Waals) forces between molecules in the surface and those in the bulk medium, imparts a free energy to the molecules in the surface (interfacial free energy) that manifests as a surface tension. For thermodynamic equilibrium this free energy is minimised which implies that the surface area is a minimum for the constraints imposed. The air-water interface has a surface free-energy of $\sim$80 mJ/m^2, whilst the oil-water interface has free-energy of $\sim$50 mJ/m^2.

Surfactactants are amphipathic molecules; one region of the molecule is polar and hydrophilic whilst the other is non-polar and hydrophobic. These molecules will preferentially locate at an oil water interface and greatly reduce the interfacial tension between the bulk media.

Lipids are amphipathic molecules and are a major component of all cell membranes. There are numerous different kinds of lipid molecules but they all share the feature of a hydrophobic non-polar tail and a hydrophilic, polar, head group. An example of such a lipid molecule (lecithin or phosphatidyl choline) is is shown in Figure 2. It is a widespread constituent of the membranes of living cells.

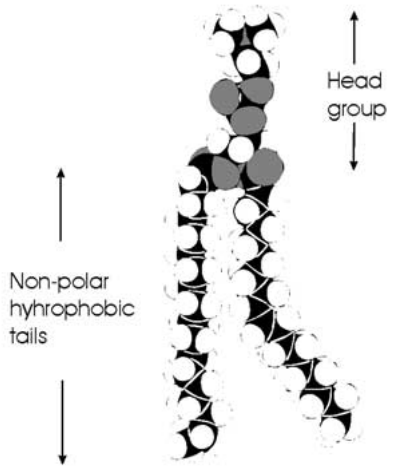

Figure 2. A model of the lecithin molecule. The polar head region for lecithin contains a trimethyl-ammonium-phosphate zwitterion. The hydrophobic tails frequently have at least one double bond partway along the chain.

The packing of lipids such as lecithin at a hydrophobic-hydrophilic interface and the effects on the interfacial free energy can be studied using a 'Langmuir trough'. Such a system is shown schematically in Figure 3. It consists of a tray containing water (or other fluid) in which the surface is divided into two areas by a moveable barrier. The barrier is attached to one of the fixed sides by a fine spring and a means of measuring the tension in this spring. A 'film' of amphipathic molecules can be formed at the air-water interface by the addition of a small amount of the amphipathic substance such as a lipid, to the system. Such a film is referred to as a Langmuir-Blogett film (after the original researchers [12]).

If the lipid molecules are added only to one side of the barrier (see Figure 3), an imbalance in the surface free-energy (surface tension) will cause the barrier to be drawn to the left until the tension in the spring counterbalances the difference in the surface tension in the two areas; see Figure 4.

The surface pressure, $\pi = \gamma_{W}\text{-}\gamma_{WS}$, which is the difference between, for instance the air-water and the air- lipid-water interfaces, will depend on factors such as the area density of lipid molecules in the interface as well as the temperature. The area available to a given number of lipid molecules can be varied by moving the barrier in the Langmuir trough. It is then possible to plot the surface pressure as a function of area. The general form of such isotherms is shown in Figure 5.

These isotherms are reminiscent of the isotherms for gases, including the notion of condensation and critical points. For small values of the area (for a fixed number of lipid molecules) the surface pressure at low temperatures rises very steeply. This corresponds to the point where the lipid molecules are close packed; any further decrease in area requires the lipid to move out of the interface into either the bulk water medium or air.

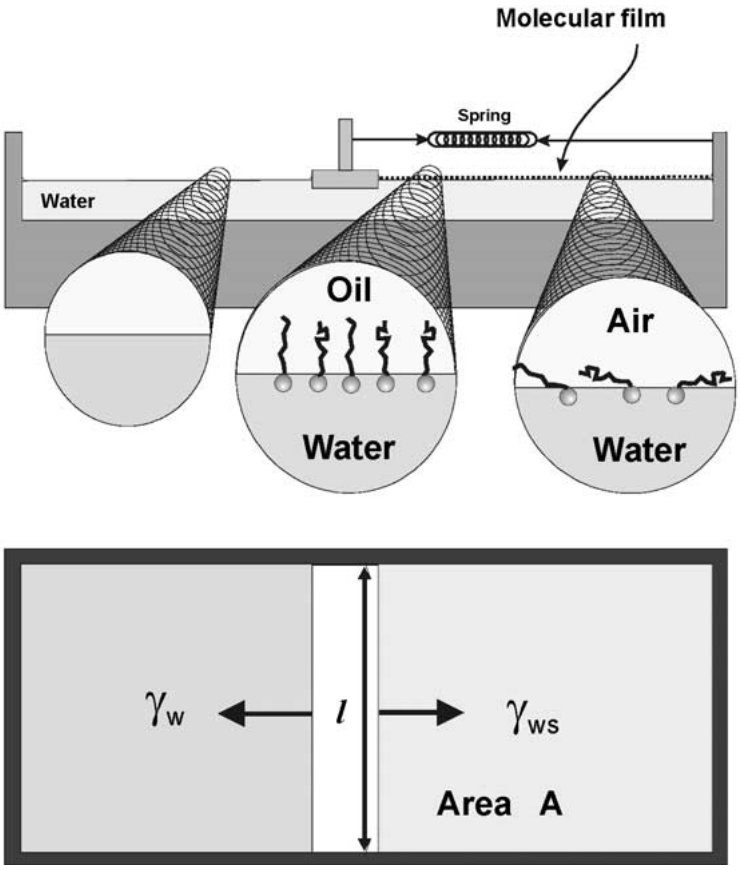

Figure 3. A schematic diagram of a Langmuir trough. The trough here is shown filled with water on which a monolayer of amphiphilic molecules is present at the air-water interface in the right half of the trough. The latter is separated from the left part by a moveable barrier. The force required to maintain the position (shown schematically by the spring) of the barrier provides a measure of the 'surface pressure' of the molecular film. When the surface density of the amphiphiles is large (middle enlarged inset), the hydrophobic tails are constrained to orient towards the normal to the surface. At low surface densities (right enlarged inset), the hydrophobic tails of the amphiphiles can lie almost parallel to the surface.

When dispersed in water, lipid molecules tend to form aggregates. Several forms of the aggregates are possible, depending on the relative dimensions of the polar head groups and non-polar tails. This is illustrated in Figure 6. When lecithin (phosphatidylcholine) is dispersed in water, it can form spherical micelles, vesicles and bi-molecular membranes. These aggregates form spontaneously.

The lipid bilayer structures which form the basic matrix of cell membranes, represent a balance between the attractive forces that minimise the contact between the hydrophobic portions of the lipid molecules and water and the repulsive forces between the lipid molecules (which becomes more significant as the spacings be-

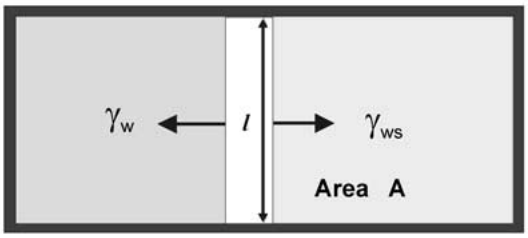

$$\textit{Net Force} \quad F = l \cdot \gamma_w - l \cdot \gamma_{ws}$$

$$\textit{or} \quad \frac{F}{l} = \gamma_w - \gamma_{ws} = \pi_s \quad (\textit{surface pressure})$$

Figure 4. Schematic of the plan view of a Langmuir trough with amphiphilic molecules spread on the surface on the right side of the barrier. The reduced interfacial tension on that side of the moveable barrier provides a 'surface pressure'.

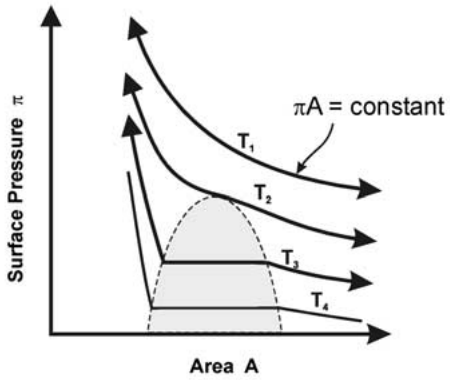

Figure 5. Isotherms of the surface pressure, π, as a function of the area available to the amphiphilic molecules at various temperatures. At very high surface densities (low values of area for a given number of amphiphilic molecules) the surface pressure rises very rapidly. This occurs when the molecules are essentially close-packed and any further reduction in area requires molecules to be pulled out of the interface. The isotherms are the 2D equivalent of the PV isotherms for a gas.

tween the lipid molecules decreases). With reference to Figure 7, the interfacial tension for aggregates such as a lipid bilayer membrane can be deduced from the following:

$$\text{At minimum } \frac{dE}{da} = 0 \quad a = a_0$$

$$\textit{i.e. } a_0 = \sqrt{\frac{c}{\gamma_{ow}}}$$

$$\text{with } \pi = \gamma_{ow} - \gamma, \quad \pi(a - \alpha) - kT$$

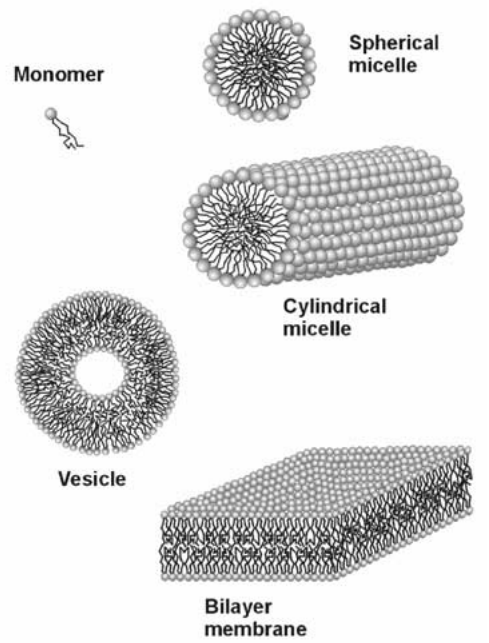

Figure 6. Possible aggregates of lipids. In the aggregates, the hydrophobic energy is minimised by reducing the contact between water and the hydrocarbon tails of the lipids. Other factors that enter into the formation of the different types of aggregates are the packing constraints for the lipid molecules and the balance between entropy and energy of the various possible states of aggregation.

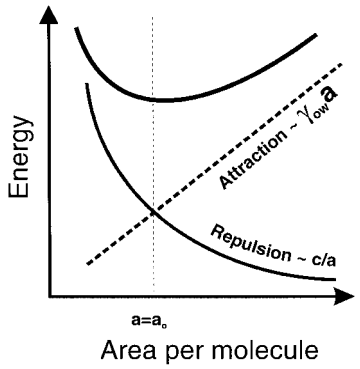

Figure 7. The lipid spacing and packing in an aggregate of lipids such as a lipid bilayer, is determined by a balance between the attractive and repulsive forces.

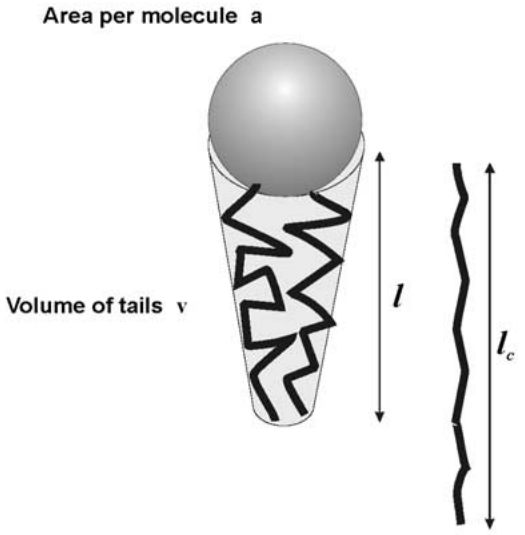

Figure 8. Packing constraints for lipid molecules. For a given area available per lipid, the hydrocarbon tails can be packed into a volume, v, which is determined by the length, l_c, of the extended chain(s) and the head group area.

$$\text{hence } \gamma = \gamma_{ow} = \frac{kT}{a - a_0 + \frac{kT}{\gamma_{ow}}}$$

1.2 Packing Constraints

For many lipids, the hydrophobic acyl chain is flexible and can take up many configurations, depending on the geometry of the aggregate in which it is located. The hydrophobic portion, however, occupies a largely fixed volume and the projected area of the polar group likewise has a specific value (although the latter may vary depending on the orientation of charged or zwitterionic entities that make up the polar head group. This is illustrated in Figure 8. These geometrical constraints impinge on the type of aggregate that the lipids can form [13]. Thus for a:

$$\text{Spherical micelle: } \frac{v}{a} = \frac{4\imath l^3}{4\pi l^2} = \frac{l}{3}$$

$$\text{Cylindrical micelle: } \frac{1}{3} < \frac{v}{a_0 l_c} \leq \frac{1}{2}$$

$$\text{Lipid bilayer: } \frac{v}{a_0 l_c} \rightarrow 1$$

Where:
l_c is the length of the extended acyl chain(s),

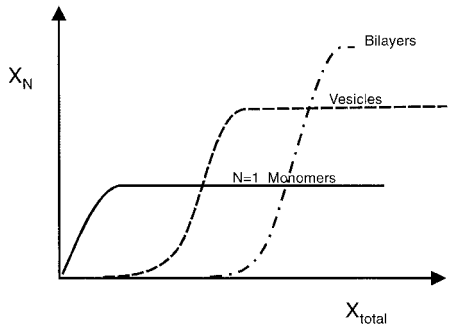

Figure 9. Lipid dispersions in water give rise to a mixture of lipid aggregates. Micelle aggregates of the lipid appear at high concentrations of the monomer. When the micelles form, addition of further lipids does not increase the concentration of the monomers in solution but drives the equilibrium to the further formation of micelles (each containing N monomers). When the micelle concentration is very high, bilayer aggregates form.

v is the volume (condensed) occupied by the acyl chains,
a_0 is the area per head group.

1.3 Thermodynamics of Aggregates of Lipids

On dispersion of the substance in water, the concentration of the monomer initially simply rises with increases in the material added. However, at some stage micelles begin to form and additional lipid added to the mix then does not lead to an increase in the concentration of the monomer molecules; instead the concentration of micelles rises, see Figure 9. At high concentrations of micelles, other aggregates such as those shown in Figure 6 appear.

The condition for equilibrium between the molecules in the aggregates and the monomers is that the chemical potential for the molecules in these two states must be the same. The chemical potential will contain entropy terms that are dependent on the concentration or mole-fraction of the lipids as well as energy terms that are *independent* of their concentration. For example, if we consider the case of a spherical micelle containing N lipids in equilibrium with the mono-dispersed lipids, we have:

$$\mu_1 = \mu_s$$

or

$$\mu_{1.0} + \mathrm{kT} \ln \mathrm{X}_1 = \mu_{s,0} + \frac{\mathrm{kT}}{\mathrm{N}} \ln \frac{\mathrm{X_S}}{\mathrm{N}} \tag{6}$$

where $\mu_{1,0}$ and $\mu_{S,0}$ are the standard chemical potentials for the monomer and the spherical micelles each containing N lipids (N-mers) respectively. These terms include all the contributions that are *independent* of the concentration.

X_1 is the mole fraction of the monomers and X_S is the mole fraction of lipids tied up in the spherical micelles (N lipid molecules per micelle); the mole fraction of aggregates, considered as a combined molecular entity is therefore X_S/N.

In equation (6), the terms in X represent the entropy expressed per molecule; for the aggregate (N-mer) this is the 'communal' entropy expressed per molecule in the aggregate.

The lipids in a bilayer aggregate are similarly in chemical equilibrium with the lipid monomers. However, for the lipid bilayer aggregates it is possible to identify a Free-energy term which derives from the form of the aggregate; the interfacial free energy of the surface of the membrane in contact with the aqueous medium. This free energy can be included explicitly as a separate term from the standard chemical potential. The intefacial Free-energy is a parameter that plays an important role in determining the stability and electrical properties of the membrane as we will see later. For a macroscopic area of a lipid bilayer, the number of lipids, N, in such a piece of membrane is very large. The entropy per lipid molecule (the second term on the right hand side in equation 6) in the lipid membrane is therefore negligibly small. Thus the equilibrium condition for the lipid bilayer can be simplified to:

$$\mu_{1,0} + \mathrm{kT} \ln \mathrm{X}_1 = \mu_{m,0} + \gamma_m \mathrm{a} \tag{7}$$

where:
γ_{m} is the interfacial free energy per unit area and
a is the surface area per molecule
$\mu_{m,0}$ is the standard chemical potential for the lipids in the membrane

For artificially constructed lipid bilayers, γ_{m} is of the order of 1–2 mJ/m^2 [14] and thus much smaller than the $\sim$50 mJ/m^2 for the interfacial free energy for the oil-water interface.

1.4 Artificial Lipid Bilayers

Bimolecular lipid membranes can be constructed in the laboratory as follows. Lipids are dispersed in a hydrocarbon solvent such as hexadecane and a film of this mixture is made across an aperture in a septum dividing two aqueous electrolytes; see Figure 10. The film may be produced in a variety of ways (e.g. see [15]) such as brushing the hydrocarbon-lipid mixture across the aperture with a fine brush or creating a film using a syringe by wiping the chamfered face of the hyperdermic needle across the aperture. A lipid monolayer then forms at the two hydrocarbon (oil)-water interfaces. The hydrocarbon solvent between these two interfaces drains out in time (upwards because the hexadecane is buoyant). The film of alkane solvent is of the order of a wavelength of light in thickness, which can be ascertained by the coloured interference bands that appear. As the alkane solvent continues to drain out, the film thins and eventually the two monolayers coalesce in one region (usually the lower, thinnest region of the film) and form a bimolecular layer. This thickness of this bimolecular layer is much smaller than

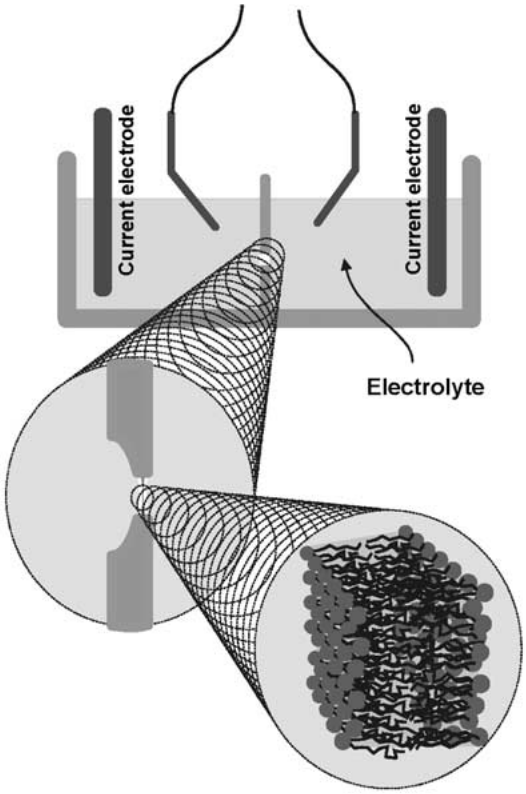

Figure 10. Experimental set-up for making planar lipid bilayers. The lipid bilayers are generated across an aperture in a polymer septum that separates two aqueous electrolyte solutions. The set-up allows measurement of the electrical and dielectric properties of the membrane via electrodes in each chamber.

the wavelength of light and therefore appears 'black'[1] as the light reflected from the membrane water interface undergoes a phase change whilst that reflected from the front interface (water-membrane) does not. The 'black', bimolecular region gradually grows in area as the alkane solvent is squeezed out of the film by the Van der Waals compressive forces until eventually the entire area of the aperture is 'black'. The process can be clearly seen in the series of photographs shown in Figure 11. When the entire aperture appears 'black', the presence of the bilayer can be detected by monitoring the electrical conductance and/or capacitance; the electrical conductance of the lipid bilayer is extremely low.

[1] For this reason bimolecular lipid membranes or lipid bilayers are often referred to as 'black' membranes.

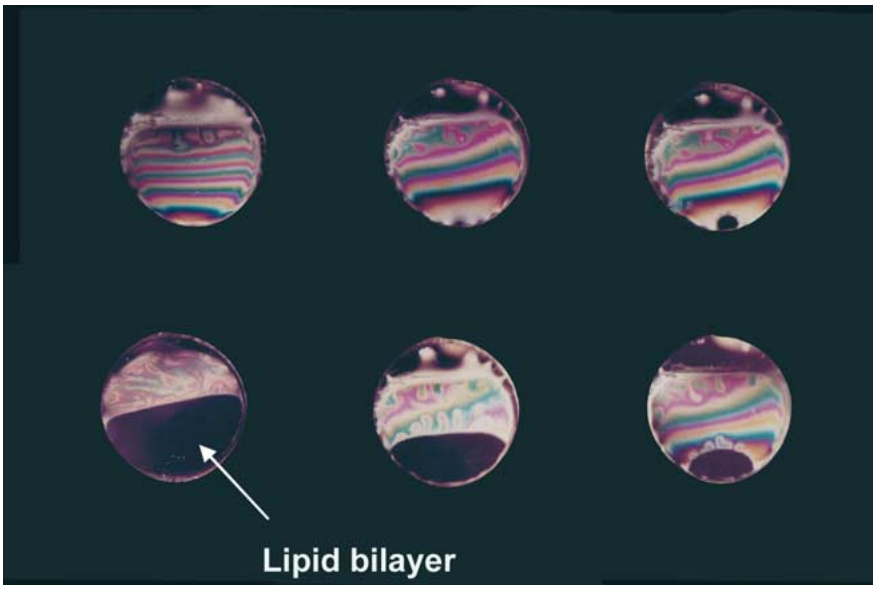

Figure 11. Formation of a lipid bilayer across an aperture of a septum in an experimental chamber as shown in Figure 10. Initially a thin film of a hydrocarbon solvent containing the lipid is generated across the aperture (first two frames, top row). The film at this stage has a thickness of the order of a wavelength of light as can be noted from the formation of coloured interference fringes. As the film thins further by drainage of the hydrocarbon solvent from the film (upwards because the hydrocarbon solvent is buoyant), a small black patch appears (usually at the bottom of the film). This patch has a thickness much less than the wavelength of light – hence its black appearance. The hydrocarbon solvent then gradually diffuses and is squeezed out of the film until eventually the entire area of the aperture is covered by a 'black' membrane. The presence of the membrane is easily monitored, even though it is difficult to see, because it has a very large electrical impedance. Photographs by the late Dr Chris Karolis at UNSW (PhD thesis, UNSW 1993).

PART 2: ELECTRICAL PROPERTIES

2.1 Electrical Conductance

The experimentally measured conductances for artificial lipid bilayer membranes are indeed very low; of the order of 10^{-3} S/m^2 [16], which makes it a better insulator than a layer of glass of comparable thickness. Whilst it has a very low electrical conductivity, two dimensional it is a very flexible, fluid.

Lipid bilayers have a central, non-polar, layer that is about 2–3 nm in thickness. Ions do not readily partition into the lipid membrane; not because the structure is tight but due to the fact that there is a very considerable energy cost associated with transferring an ion from a medium of high dielectric constant, such as water, to one of low dielectric constant, such as the central region of the lipid bilayer. The hydrophobic region of the lipid bilayer has a dielectric constant of $\varepsilon_m \sim 2.1$ [[16–20] whilst the aqueous medium has a dielectric constant of $\varepsilon_w \sim 78$. The

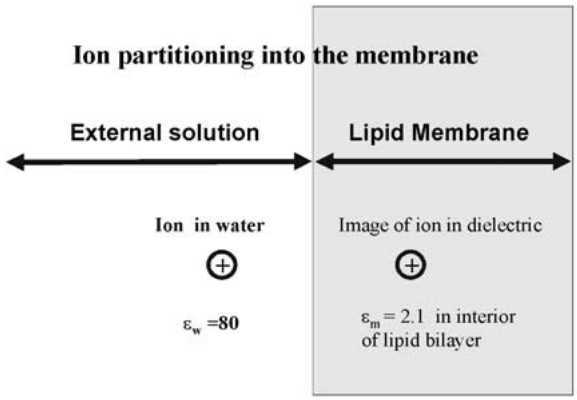

Figure 12. Ion partitioning into the membrane is determined by the relative 'self-energies' of the ions in the two media (water and lipid). The field energy of an ion is dependent on the dielectric constant of the medium. The difference in the electrostatic field energy in the two media is known as the Born energy. The latter can be also determined from the electrostatic repulsive force between the ion and its images in the lipid medium that arise from differences in the dielectric constant between the two media.

partitioning of ions from the aqueous solution into this layer can be deduced from the electrical image forces which arise as ions approach the membrane from the aqueous medium, see Figure 12. The electrostatic image forces are related to the differences in the self-energy of an ion in the two media (lipid and water). The self-energy of an ion is simply the energy stored in the electric field of the ion. Thus for an ion of radius R in a medium of dielectric constant ε_1 and infinite extent, the electrostatic self-energy, W_1, is;

$$W_1 = \int_{r=R}^{r=\infty} \frac{1}{2}\varepsilon_1\varepsilon_0 E^2.4\pi r^2 dr \tag{8}$$

where the field, $E = \dfrac{z \quad e}{4\pi\,\varepsilon_1\varepsilon_0 r^2}$.

The difference in the self energy of an ion in the lipid bilayer interior and aqueous media, referred to as the Born energy [21, 22] for ion partitioning is thus given[2] by:

$$W_B = \frac{z^2e^2}{8\pi\,\varepsilon_0 R}\left[\frac{1}{\varepsilon_m} - \frac{1}{\varepsilon_w}\right] \tag{9}$$

[2] The lipid bilayer is very thin and the calculation of the self-energy for an ion situated at the centre of the bilayer is therefore somewhat more complicated compared to that of an infinite medium. A full analysis of this problem has been presented by Neumcke and Läuger [22]. This analysis shows that the self-energy rise very steeply as the ion enters the membrane and reaches a value very close to that expected for a medium of infinite extent. This is, in retrospect, not unexpected as the field energy density around an ion falls off as $1/r^4$.

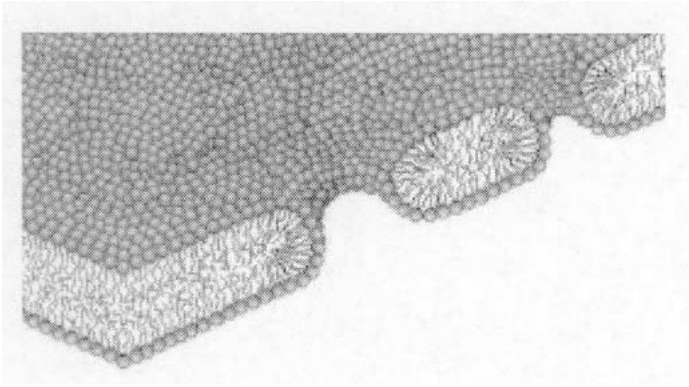

Figure 13. Pore 'defects' in a lipid bilayer. The pores envisaged provide aqueous connections between the solutions on the two sides of the bilayer (based on [23]).

where: R is the radius of the ion
e is the electronic charge
z is the valency of the ions
ε_{m} is the dielectric constant of the membrane interior
ε_{w} is the dielectric constant for water
ε_0 is the permittivity of the space

For a potassium ion, the Born energy for partitioning into the central non-polar region of a lipid bilayer is of the order of 3eV [23]. The concentration of ions in the interior of lipid bilayers for such an ion is therefore extremely small; at room temperature the ions would partition in the ratio $\mathrm{e}^{-3/0.025} \sim \mathrm{e}^{-120}$ between the aqueous solution and the membrane interior!

Thus while the membrane is very fluid and the mobility of ions in the membrane may be quite high, the electrical conductance of the lipid bilayers remains low because there are so few ions to carry the current. The conductances of lipid membranes determined experimentally are indeed very low but surprisingly are still much larger, by some twenty *orders* of magnitude, than that predicted from the very low concentrations of carriers in the lipid membrane! This points to another mechanism for electrical conduction through lipid bilayer membranes.

2.2 Formation of Pore Defects

So far we have considered lipid bilayers which contain no transmembrane connections between the two aqueous phases which it separates. Pore structures like the that shown in Figure 13 may form, however, in the lipid bilayer [24–26]. A cross sectional view of the putative pore is shown in Figure 14a. These pores provide an aqueous conduction pathway through the lipid bilayer and thus contribute significantly to the electrical conductance of the membrane. It is useful to examine

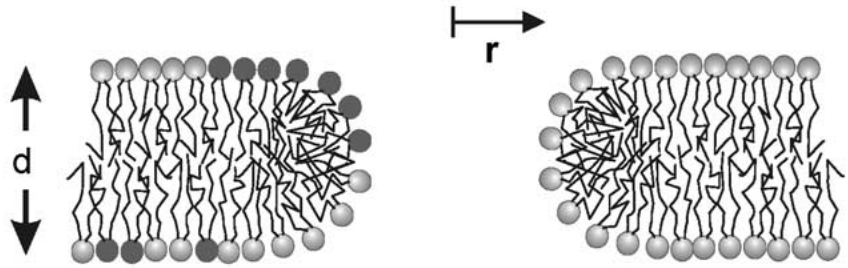

Figure 14a. A cross section of the pores illustrated in Figure 13. To accommodate the volume occupied by the tails of the lipids in the curved portions of the pore, the lipid head groups are required to be spaced further apart.

the thermodynamics of the formation of such pores and some of the properties associated with them.

The curved surface of the pore is lined with lipid molecules but the reduced volume available to the tails of the lipids in the curved regions of the pore impose packing constraints on the lipid molecules which require the lipids head groups to be spaced further apart than in the planar part of the bilayer. Essentially this leads to a greater hydrophobic interaction since the water molecules near the membrane surface will now penetrate further, on average, into the non-polar constituents of the lipid structure. A good first approximation of the increase in the surface free energy in these curved regions in the pores can be deduced from the increased surface area per molecule and assuming a surface free energy per unit area similar to that of an oil-water interface. Thus, with reference to Figure 14a, for a pore of radius r, the energy required to create the curved surface is:

$$\mathrm{W_P} = \left(2\pi r \frac{\pi \mathrm{d}}{2}\right) \gamma_P = \pi^2 \mathrm{r\ d}\gamma_P \tag{10}$$

where γ_{p} is the surface free energy per unit area in the curved regions of the pore and is expected to be larger than the interfacial free-energy for the planar surfaces of the bilayer.

The energy cost of creating the curved surface of the pore is offset by the energy saved from not forming the disc of planar bilayer that was present before the pore was formed. This energy is simply $2\pi \mathrm{r}^2 \gamma_{\mathrm{m}}$. The net cost of creating a pore of radius r is then given by:

$$\mathrm{E_P} = \pi^2 \mathrm{rd}\gamma_P - 2\pi \mathrm{r}^2 \gamma_m \tag{11}$$

Figure 14b illustrates the dependence of $\mathrm{E_p}$ on radius. Initially the net energy cost of creating a pore increases with the radius of the pore, but reaches a peak at a radius $\mathrm{r}=\mathrm{R_c}$, after which the energy cost decreases with further increases in the pore radius. We will return to this later.

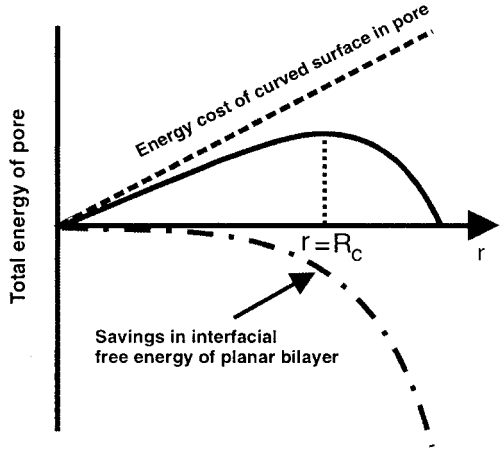

Figure 14b. The energy of forming a pore as a function of pore radius. The two contributions to this energy are the energy cost of creating the, curved, surface of the pore itself (which increases with the perimeter length and hence linearly with pore radius) and the saving in energy that results from not creating the area of the planar bilayer that otherwise would have occupied the space. At the critical radius R_c, the energy of forming a pore has a maximum value and any pore with this radius would grow spontaneously in size.

Now that we have the energy required to form a pore we can determine, at least the relative, probability of formation of pores of different radii using the Boltzmann distribution function.

2.2.1 ELECTRICAL CONDUCTANCE OF PORES IN LIPID BILAYERS

The electrical conductance of the pores will dominate the overall conductance of the membrane since the conductance of the bilayer itself is extremely low. The conductance of a pore filled with water will depend on the concentration of ions in the pore. The latter will be smaller than that of the bulk electrolyte solutions since there remains an energy cost to insert an ion into a narrow aqueous pore in the bilayer (which has a low dielectric constant). The Born energy for partitioning can again be calculated from the energy stored in the electric field (self-energy) although the calculation is considerably more complicated when the field of the ion distributed between two different media and the spherical symmetry is lost. The Born energy will depend on the shape and size of the pore. For simple geometries such as a long, narrow, cylindrical pore, the Born energy for partitioning is given [27] by:

$$W_B = \frac{z^2 e^2 \alpha}{4\pi r \varepsilon_0 \varepsilon_w} \tag{12}$$

where:
z is the valency of the charge carriers (ions)

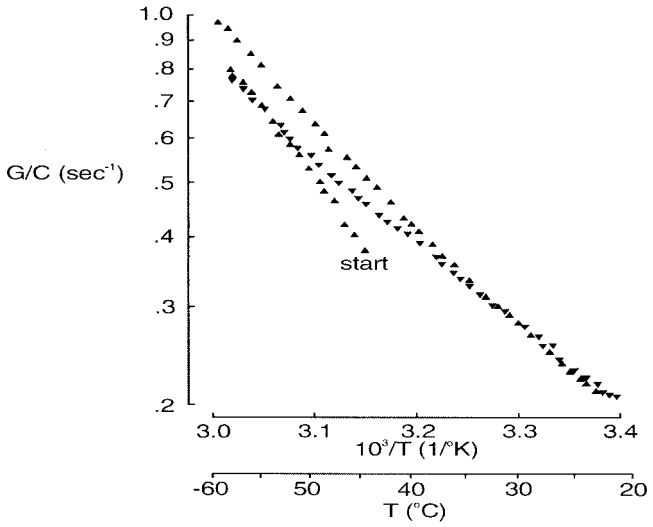

Figure 15. An Arrhenius plot of the conductance of a lecithin-cholesterol lipid membrane in a 1 mM KCl solution, normalised with respect to the area of the bilayer (by normalising with respect to the bilayer capacitance which is proportional to its area). The series of measurements were made continuously as the temperature was increased (▲) and then decreased (▼) and then raised again. The final slope the activation energy for conduction gave a value of 38 kJ/mole (from ref. [28]).

e is the electronic charge
α is a form factor and for a cylindrical pore [27] has a value $\sim$0.175
r is the radius of the pore
ε_w is the dielectric constant of water
ε_o is the permittivity of free space

The total conductance of the membrane will be determined by the number of pores and the distribution of pore sizes (which will determine the distribution of pore conductances).

Measurement of the electrical conductance as a function of temperature can be used to obtain an activation energy for the conduction process. This activation energy will contain two contributions [28]:

(i) An activation energy for diffusion through the aqueous pore ($\sim$18 kJ/mole).
(ii) The energy for partitioning ions into the pore.

The electrical conductance and the activation energy for conduction can be measured using the experimental set-up shown in Figure 10; the electrical impedance [16, 29][3] can be measured using a 'four terminal' method. An example [28] of such a measurement for Lecithin-Cholesterol bilayers (2:1 ratio) is shown in Figure 15.

[3] In 'four terminal' techniques the current is injected into the system via two electrodes and the potential developed across the membrane is measured with two additional electrodes. The measurements of the potential difference developed across the bilayer are made with amplifiers of very

These results yielded an activation energy for conduction for these lipid bilayers of ~38 kJ/mole.

On the assumption that the diffusion of ions in the pore will be very similar to that of a free solution (mobility $\sim 2.\ 10^{-9}$ m^2/s), the activation energy for diffusion through the aqueous medium in the pore is ~18 kJ/mole. The remaining 20 kJ/mole of the energy of activation contains two components;

(a) the Born energy of partitioning of the ions into the pore (image forces),
(b) the temperature dependence of the average pore size (and perhaps the number of pores).

From the Born energy for partitioning of the ions into the pore, it would be possible to calculate the radius of the pores on the assumption that the conduction occurs through pores of simple geometry. However, the two contributions to the activation energy (a) and (b) referred to above are difficult to separate. Some useful insights can be obtained by assuming the activation energy to derive solely from the Born image forces. Using the value of the partition coefficient for the ions determined by the Born energy (equation 12), the average radius of an equivalent cylindrical pore and its conductance then can be calculated. From the average conductance of a pore, we can also calculate the total number of pores required to account for the total measured conductance. This yields the following values:

Pore radius: ~1.1 nm; Number of pores per m^2: $\sim 10^{10}$.

The pores completely dominate the electrical conductance of the lipid bilayer membrane but they occupy only 2.10^{-7} of the total area.

2.3 Membrane Stability

As pointed out earlier, the energy of formation of pores is a function of pore radius. Initially the energy cost of creating a pore increases with pore radius. Beyond a critical radius R_c, however, the energy cost begins to decline with increasing radius. Pores with a radius greater than this critical radius will therefore grow in size uncontrollably which would lead to the eventual rupture of the membrane.

From equation (11), the maximum energy for the formation of a pore occurs when $\frac{\partial E_P}{\partial r} = 0$ (see also Figure 14b). This corresponds to a critical pore radius, R_c, given by:

$$R_c = \frac{\pi d.\gamma_P}{4\gamma_m} \tag{13}$$

The energy of a pore of this radius is:

high input impedances ($\sim 10^{14}$ ohms), and hence the potential drop across the electrode-electrolyte interface will be negligibly small for the potential-measuring electrodes. The separate measurement of the membrane potential difference and current passed through the membrane allows the impedance of the bilayer to be determined. The conductance can be also measured using AC currents. It has been shown by these authors, that the conductance measured at a frequency of ~1Hz largely reflects the conductance of the central hydrocarbon region of the bilayer.

$$E_c = \frac{\pi^3 (d.\gamma_P)^2}{8\gamma_m} \tag{14}$$

As we noted, a pore with a radius equal to the critical radius will grow uncontrollably and would eventually lead to the rupture of the membrane. In a cell, if the lipid bilayer was not 'pinned' by intrinsic and extrinsic membrane proteins, this would cause lysis of the cell.

2.3.1 EFFECT OF LIPID COMPOSITION

The lipid bilayer components of cell membranes contain a mixture of lipids. Artificial lipid bilayers can also be made from lipid mixtures. The nature of the lipids would be expected to influence the formation of the pores discussed above, in the following manner.

Lipid molecules which have a smaller volume of non-polar components or relatively larger polar heads would be expected to pack more readily into the curved region of the pore since that would reduce the exposure of the hydrophobic region of the structure to the aqueous medium. This would decrease the surface free energy in the curved surface of the pore. In turn this would decrease the critical pore energy and critical pore radius. A form of lecithin exists that has only one hydrocarbon-chain tail (but the same trimethyl amonium-phosphate group polar head). This lipid would be expected to favour the formation of pores and it is interesting to note that this lipid promotes the lysis of cells and is referred to as *lysolecithin*. Conversely, molecules such as cholesterol, which are found in all mammalian cell membranes and which have a very small polar head (a single OH group) and a bulky hydrophobic part, would have an inhibiting effect on the formation of pores. Indeed, in experimental studies on lipid bilayers cholesterol is often included as it greatly increases the stability of lecithin bilayers. It also decreases the electrical conductance of the membranes [30].

2.4 Effect of Trans-Membrane Potentials on Pore Defects

One of the ubiquitous features of living cells is the presence of an electric potential difference between the cytoplasm and the exterior medium. This potential difference appears across the cell membrane and typically has a value of around 60 mV; it ranges from $\sim$10 mV in erythrocytes (red blood cells) to $>$250 mV in some aquatic plant cells. The cytoplasm is always negative with respect to the external medium.

A value of the potential difference of $\sim$60 mV across a membrane which is $\sim$6 nm thick represents an average field strength in the membrane of $\sim 10^7$ V/m. This is a very large field strength. Further, as this is an average value of the field strength across the 6 nm structure, the field strength in individual regions of the membrane such as the central hydrophobic region of the lipid bilayer, is likely to be much larger than this.

The membrane is very thin and has therefore a significant capacitance; typically around 10^{-2} F/m^2. The electrical energy stored in the membrane capacitance at a membrane potential of 60 mV is therefore $\sim 1.8 \times 10^{-5}$ J/m^2. That figure is considerably smaller than the 1–2 $\times$ 10^{-3} J/m^2 for the interfacial free energy (without any contribution from the electrical energy). However, while the electrical energy stored may be small compared to the total interfacial free energy at physiological membrane potentials, the membrane potential may feature significantly in the formation of pores in the lipid bilayer membrane.

In order to simplify the analysis we will limit our discussion initially to pores that are small compared to the Debye length for the surrounding medium. If a potential difference is applied across the membrane, the potential profile in the vicinity of the pore will not be significantly perturbed, provided that the pores are very small (compared to the Debye length). The capacitance per unit area in the pore itself which is filled with water of dielectric constant $\sim$78, is considerably larger than the area specific capacitance of the lipid bilayer. The electrical energy stored is therefore altered (increased) when a pore is formed. However, the increase in charge stored and increase in energy stored when the pore forms must be supplied by the external emf source that maintains the potential difference across the membrane. The net result is that the *Free Energy* of the system, membrane plus source of emf, *decreases*[4].

When a potential V_m is applied across the membrane, we must include the electrical energy $\frac{CV_m^2}{2}$ where C is the capacitance (per unit area). The capacitance, per unit area, will be much larger for the pore than for the remainder of the bilayer. The formation of a pore of radius r (assumed to be much less than a Debye length) will therefore lead to a change in the electrical energy given by:

$$\Delta E_e = \pi r^2 \left(\frac{(C_m - C_p) V_m^2}{2} \right) \tag{15}$$

where C_m is the capacitance of the lipid bilayer (per unit area) and C_p is the capacitance (per unit area) of the water filled pore. Note that $C_m \ll C_p$.

The total energy of the pore itself is therefore given by:

$$E_P = \pi^2 r d . \gamma_P - 2\pi r^2 \left(\gamma_m \frac{C_p - V_m^2}{4} \right) \tag{16}$$

The critical radius when $\frac{\partial E_P}{\partial r} = 0$ is then:

$$R_c = \frac{\pi d . \gamma_P}{4 \left(\gamma_m + \frac{(C_p - V_m^2}{4} \right)} \tag{17}$$

[4] The charging of a capacitor from a battery decreases the overall energy in the system which comprises the battery plus the capacitor, though the energy stored in the capacitor increases.

In living cells, the potential difference between the cytoplasm and the external medium arises from both diffusion of ions due to concentration differences which are maintained via energy-driven ion 'pumps' and by energy-driven electrogenic ion transport.

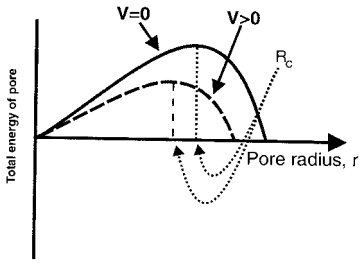

Figure 16. The effect of a potential applied across the lipid bilayer membrane on the energy of formation of pores. The critical radius for rupture decreases with increasing applied potential.

The energy to form such a critical pore is then given by:

$$E_c = \frac{\pi^3 (d.\gamma_P)^2}{8\left(\gamma_m + \frac{(C_p - V_m^2}{2}\right)} \tag{18}$$

The critical radius and the energy to form such a critical pore, which would lead to rupture, is thus decreased with increasing transmembrane potential (Figure 16). The probability of such a pore forming (via the Boltzmann probability function) thus will rapidly increase with increasing membrane potential.

Another way of looking at the effect of an applied potential on the formation of pores is in terms of a process by which water is drawn into the pore. Since the dielectric constant of water is higher than that of the interior of the membrane, the water will tend to be drawn into the high field region inside the pore. This is illustrated in Figure 17. The water is drawn into the pore by dielectrophoretic forces and this process is opposed only by the net energy costs of creating the pore in the membrane due to interfacial free energy terms.

For large pores (with a radius much larger than the Debye length), the membrane potential difference in the central portion of the pore will collapse. In those regions therefore there will not be any contribution to the electrical energy and the energy stored actually slightly decreases from that of the bilayer itself; the total *Free Energy* of the system (including the source of emf) would slightly *increase.* However, the peripheral region of the pore (within an annular ring of width equal to ~a Debye length of the perimeter) would continue to contribute to the Free Energy as before, although the functional dependence on the radius will then vary as r and not as r^2.

PART 3: PROTEINS IN MEMBRANES

In the plasma membrane of living cells, various proteins are imbedded in the lipid bilayer matrix. The lipid bilayer matrix serves a number of functions in relation to these proteins, not the least of which is to provide a means for axially orienting the

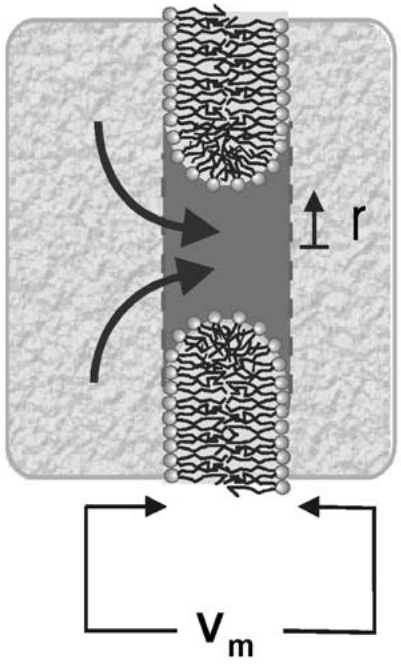

Figure 17. Dielectrophoretic uptake of water into a pore when a potential difference is applied to the membrane. The water which has a high dielectric constant is drawn into the pore where the electric field is high and displaces the bilayer material which has a low dielectric constant.

proteins relative to the normal to the membrane surface. The structure and properties of the lipid bilayer also modulate the molecular organisation and functional properties of the proteins imbedded in the membrane as we shall illustrate below.

The membrane proteins perform various specific functions and include the nanomachines which facilitate the diffusion or transport ions and other molecules against their chemical gradients, generate action potentials or are involved in signalling and effector processes such as those that are part of the immune response system.

Many membrane proteins that have been isolated and characterised are composed of several subunits that span the membrane with individual subunits interconnected by flexible strands that loop through the medium external to the membrane.

3.1 Intrinsic Membrane Proteins

All the proteins that span the membrane have a central region that is composed of amino acids that provide a largely hydrophobic surface. The two outer regions of these protein modules that reach into the aqueous environment have more polar, hydrophilic, surfaces. The exact orientation and axial positioning of the proteins in the membrane derives from a balance between opposing hydrophobic and hydro-

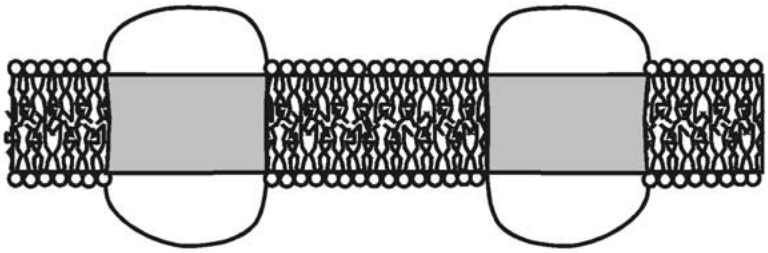

Figure 18. Protein modules imbedded in a lipid bilayer membrane have hydrophobic and hydrophilic regions. The position of the proteins minimises the interfacial free energies resulting from interactions between the polar and non-polar portions of the protein and those of the lipid bilayer and the aqueous solution.

philic forces between the non-polar membrane interior, the aqueous environment, and the polar and non-polar portions of the protein. This is illustrated in Figure 18.

We have noted that the lipid bilayer membrane is a very good electrical insulator, despite the presence of pore 'defects'. The protein modules imbedded in the lipid bilayer in fact dominate the electrical conduction properties of cell membranes.

3.2 Protein Aggregation

For proteins inserted into the lipid membrane a mismatch between the dimensions of the non-polar region of the protein and the non-polar region of the lipid bilayer, will be associated with a hydrophobic interaction energy. The latter could be evaluated from the detailed structure of the protein which is now known for a number of functional membrane proteins.

To gain insights into the physics of this problem we can begin by noting that for those parts of the protein which have a hydrophobic surface the interaction energy will be similar to that of an oil-water interface, that is $\sim$50 mJ/m^2. Interestingly, a mismatch might induce the aggregation of the protein subunits if that results in a reduction in the area of contact between the mismatched protein and the non-polar regions of the bilayer. To illustrate how the hydrophobic energies affect the molecular organisation consider, for example, the hypothetical protein module shown in Figure 19, which is composed of three subunits. In this hypothetical protein the non-polar region of the central portion of the three subunits do not match (are larger) than the thickness of the non-polar region of the lipid bilayer. All the subunits, however, are assumed to have the same hydrophobic and polar surfaces geometries.

The exposure of the hydrophobic surfaces of the protein to the polar aqueous environment will be different for the aggregated and separated subunits. This will lead to a difference in the hydrophobic interaction energy for the separated and aggregated subunits. The condition for equilibrium between aggregates of the three

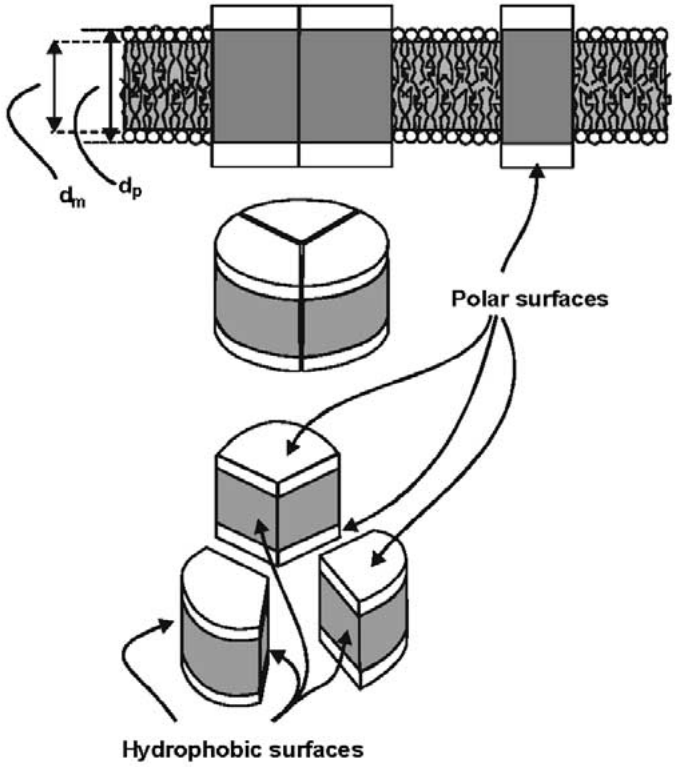

Figure 19. A hypothetical protein module made up of three subunits, imbedded in a lipid bilayer membrane. The subunits may aggregate as trimers or can be dispersed as single subunits. The equilibrium distributions of these two configurations are determined by the chemical potentials of the monomer and trimers.

subunits (trimers) and the dissociated units (monomers) is determined by the requirement that the chemical potentials for these configurations be the same.

Thus,

$$\mu_{1,0} + \mathrm{kT} \ln \mathrm{X}_1 + \mathrm{E_h} = \mu_{3,0} + \frac{\mathrm{kT}}{3} \ln \frac{\mathrm{X}_3}{3} \tag{19}$$

Where:

$\mu_{1,0}$ and $\mu_{3,0}$ represent the standard chemical potentials and contain the contributions which are not dependent on the concentration, including the hydrophobic interactions between the protein subunits and the lipid bilayer when it is in the trimer configuration; any additional difference in the hydrophobic energy is included in $\mathrm{E_h}$.

$\mathrm{E_h}$ is the additional hydrophobic free energy when the subunits are in the monomer form relative to that when they are aggregated as trimers;

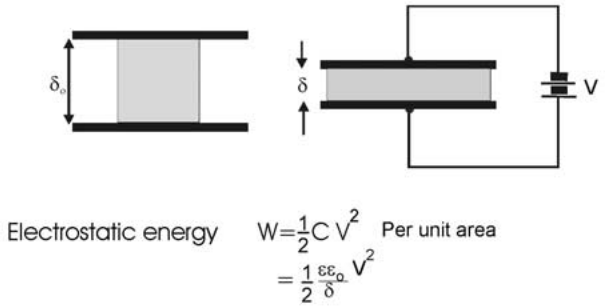

Figure 20. Electrostriction of a material in an electric field. The situation depicted in which the material in question is sandwiched between two parallel plate electrodes, is similar to the cell membrane sandwiched between two electrolyte solutions and a potential difference is maintained across the membrane.

X_1 and X_3 are the mole fractions of the protein subunits in the trimer and monomer state;

In the trimer state the inner (radial) flat faces of the protein subunits only interact with each other and, as their non-polar regions match, this does not contribute to any hydrophobic interaction. As monomers, however, these protein surfaces are exposed to the lipid bilayer matrix and the width of the hydrophobic surface of the protein does not match the width of the central hydrophobic region of the lipid bilayer. This leads to a additional interaction energy that is denoted E_h and explicitly included as a separate term. For simplicity we assume that there are no other differences in the interaction of the proteins subunits with the lipid bilayer.

It is interesting to estimate the magnitude of the difference in hydrophobic free energy of aggregation for a given, small, mismatch in the geometry of the hydrophobic surfaces and that of the lipid bilayer. Assume, for instance, that for the hypothetical protein shown in Figure 19, the hydrophobic region of the protein subunits have a width d_P = 2.1 nm whilst the bilayer is taken to have a central hydrophobic region of width, d_m = 2.0 nm. For this example the difference in hydrophobic energy between the aggregated and dissociated forms of the subunits is ~0.125 eV (or 5units of kT at room temperature).

The ratio of trimers to monomers can then be obtained directly using the Boltzmann distribution function. Thus taking $\mu_{1,0} = \mu_{3,0}$ the ratio of trimer aggregates to monomers is given by:

$$\frac{x_3/3}{(x_1)^3} = e^{\frac{3E_h}{kT}} \tag{20}$$

For the hypothetical example protein under consideration, almost all the proteins therefore will be in the trimer form; if there are 10^6 trimers in total, the ratio of subunits located in trimers to those of monomers would be ~200:1.

3.3 Effect of Membrane Potential and Homeostasis

We noted that in cell membranes a very large electric field is present as a result of electric potential differences maintained across this very thin structure. In the presence of such large electric field strengths electrostriction effects may occur, particularly in the proteins in the membrane. The compressive stress due to the electric field can be readily deduced from the dependence on the electric field energy on the thickness of membrane [31]. Thus with reference to Figure 20, the electrostriction force is given by:

$$P_e = -\frac{dW}{dx} = \frac{1}{2}\frac{\varepsilon\varepsilon_0}{\mathrm{d}^2}V^2$$

The elastic restoring force resulting from the compression of the material (assuming it behave as an ideal elastic) is given by:

$$P_m = -Y\int_{\mathrm{d}_0}^{\mathrm{d}}\frac{dx}{x} = Y\ln\frac{\mathrm{d}_0}{\mathrm{d}}$$

Here d and d_0 are the thickness of the non-polar portion of the protein subunits with and without the field respectively; Y is the elastic modulus of the proteins. The electrostriction will be almost completely confined to the non-polar parts of the proteins since most of the field appears across the non-polar part of the membrane.

At mechanical equilibrium the electrostriction stress is balanced by the elastic restoring force and hence:

$$\frac{\varepsilon_{\mathrm{P}}\varepsilon_0\mathrm{V}^2}{2\mathrm{d}^2} = \mathrm{Y}\int_{\mathrm{d}_0}^{\mathrm{d}}\frac{\mathrm{dx}}{\mathrm{x}} = Y\ln\frac{\mathrm{d}_0}{\mathrm{d}} \tag{21}$$

We saw that the aggregation of protein subunits is strongly dependent on the dimensions of the hydrophobic regions of the protein subunits and that of the lipid bilayer. The lipid bilayer itself is in a fluid state and is not very compressible (that is, its modulus for compression is very high). The latter has also been inferred from the fact that the capacitance of the lipid bilayer is essentially unaffected by an applied DC potential difference, unless the bilayer contains hydrocarbon solvents in which case the solvents are squeezed out when the field is applied and this can be monitored by measurement of its capacitance.

The proteins, however, may undergo small elastic compression as a result of the electric stress. The effects of this on the organisation of the proteins can be illustrated by considering the effect on the hypothetical protein subunits considered previously (Figure 19).

As the potential difference applied across the membrane is increased, the non-polar parts of the protein subunits will compress and may ultimately match the width, d_m of the hydrophobic region of the lipid bilayer. At that stage the hydrophobic energy of the aggregated (trimer) and monomer proteins will be the same.

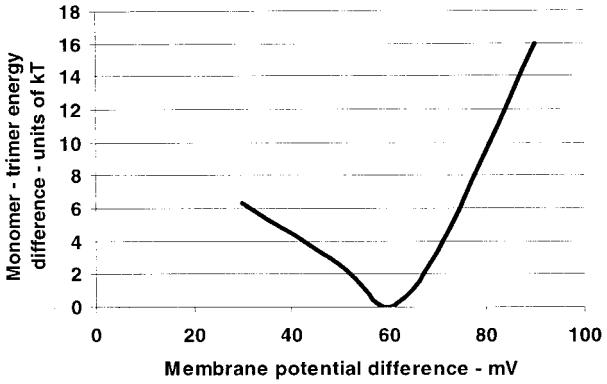

Figure 21. Effect of membrane potential on the aggregation of trimers in a hypothetical protein imbedded in a lipid bilayer. For the calculations the hydrophobic region of the uncompressed protein module, that is, at zero membrane potential, was set to 2.17 nm, the bilayer hydrophobic region to 2.00 nm, the elastic modulus of the protein to 10^6 and the dielectric constant of the protein to 20. The trimer aggregate had a radius of 2.00 nm. Note that the parameters were chosen so that at a membrane potential $\sim$ 60 mV, the electrostriction is such that the hydrophobic surface of the trimer is the same as the hydrophobic region of the lipid bilayer and hence the trimer and monomer configurations have the same hydrophobic energies of interaction.

The entropy term in Equation 19 will then ensure that the monomer configuration of the subunits will predominate (note that the mole fraction X is, by definition, < 1). Should the trans-membrane potential difference be increased further, the proteins will be further compressed and the non-polar regions of the subunits will then become smaller than the width of the hydrophobic region of the lipid bilayer. This will again lead to a difference between the hydrophobic free energy of the monomers and that of the trimer aggregate; again, this will cause an increase in the proportion of trimers compared to monomers. We can again obtain a good indication of the magnitude of these effects by assuming that the interaction energy between the polar parts of the protein and the hydrophobic region of the lipid bilayer (which they will now protrude into) is again similar to that of the oil-water interface.

An example of the variation of this ratio as a function of membrane potential for the hypothetical subunits considered earlier, is shown in Figure 21. For the purpose of this calculation, the dimensions of the non-polar region of the protein subunits were set equal to the bilayer membrane thickness d_m, when the membrane potential is equal to 60 mV. The elastic modulus, Y, was set to 10^6 (similar to that of vulcanised rubber). At membrane potential differences either smaller or larger than this the hydrophobic surfaces of the subunits would no longer match that of the lipid bilayer. The effect of that is clearly manifested in the difference in the hydrophobic energy between the monomer and trimer configurations of the subunits as shown in Figure 21. Thus, as little as a 20 mV shift from the 'set-point'

potential (of 60 mV) can change the total hydrophobic energy by some 10 units of kT.

Some of the proteins we have been considering may be ion transport systems such as ion 'pumps' that are involved in maintaining ion concentration differences which in turn determine the membrane potential. Some of these ion pumping mechanisms also involve a net charge transfer (electrogenic transport). The function of these transport systems are involved in maintaining the potential difference that is found in living cells.

If, for instance, in our hypothetical protein the trimer configuration is required for the ion transport mechanism to function, then we can see that the dependence of the aggregation on membrane potential by the mechanisms outlined provides a homeostatic control system that will maintain a set membrane potential. The latter is of importance in controlling the magnitude of nerve impulses (action potentials) and the initiation of muscle contractions *etc*. The membrane potential also plays a central role in determining the thermodynamic potentials that drive the synthesis of ATP (adenosine triphosphate) from proton gradients across membranes.

3.4 Electrical Breakdown in Cell Membranes

At the normal physiological ('resting) membrane potential ($\sim$70 mV), the electrical energy stored in the membrane capacitance is relatively small, despite the large magnitude of the membrane capacitance (typically around 10^{-2} F/m^2). This electrical energy at a membrane potential difference of 70 mV is $\sim$25 μJ/m^2 which is small compared to the interfacial free energy of a bimolecular lipid membrane (around 1–2 mJ/m^2). However, if the membrane potential is taken to 700 mV by injecting current through the membrane, the electrical energy stored becomes comparable to the interfacial free energy. This would immediately suggest that at such large, non-physiological, trans-membrane potentials the membrane might become unstable and indeed this is the case.

The electrical properties of the cell membrane for most cells can only be measured indirectly as the cells are too small to use intracellular electrodes to measure directly membrane potentials or inject current. There exist, however, some cells which are so large that it is possible to insert microelectrodes into the cells to make direct measurements of the electrical characteristics of the cell membranes.

This led to the discovery of a 'reversible electric breakdown' phenomenon[5] [38]. This was first observed in experiments in which linearly increasing currents were injeced into cells and the cell membrane potential reached sufficiently large values.

The set-up used for such experiments is shown in Figure 22.

An example of the voltage-current relationship obtained for cells of *Valonia utricularis* [32] for pulsed curents is shown in Figure 23. A striking feature of

[5] The 'reversible electrical breakdown' phenomenon first reported was also referred to as a 'punch-through' effect [38].

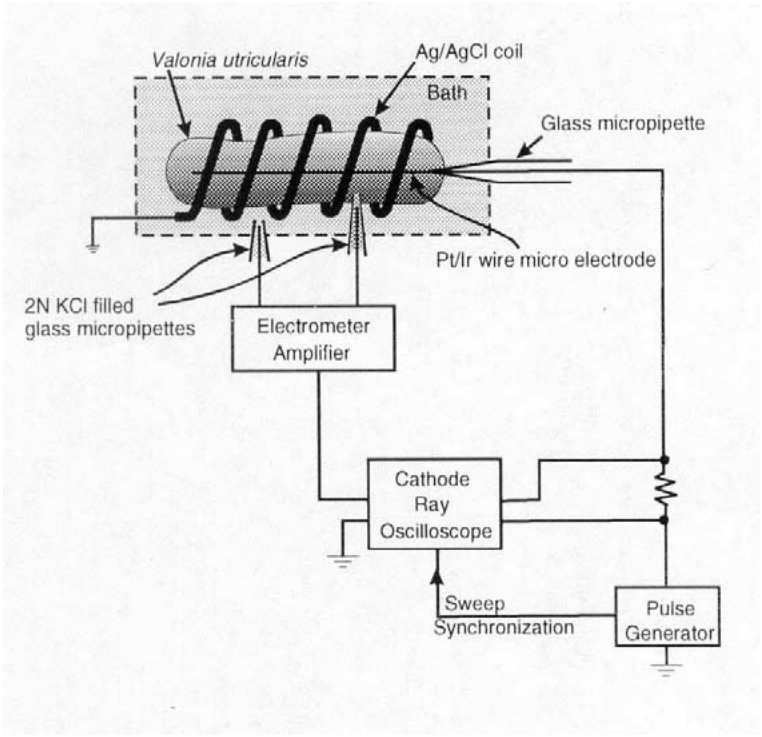

Figure 22. Diagrammatic set-up for measuring the voltage-current characteristics of cell membranes. In these experiments a metal micro-electrode is inserted longitudinally into the cell to inject current with a coil of AgCl coated Ag wire in the external bathing medium acting as the other current electrode. The potential difference between the cytoplasm and the external medium bathing the cell is measured with micro-electrodes inserted into cell and a matching electrode in the external solution. The potential measuring electrodes consist of glass micro-pipettes (tip diameter 1–10 μm) filled with 3 M KCl. Such experiments are readily performed with larger cells such as the giant axons from Squid, cells of the fresh water plant *Chara corallina*, the sea water plant *Valonia utricularis* (as is in this diagram) and others (based on [32]).

the electrical characteristics is the sharp increase in the conductivity (leading to a sharp increase in the current) at a well defined membrane potential. This is a clear demonstration of electrical breakdown of the cell membrane. The breakdown in this case did not cause destruction of the cell, and the points shown in the plot were obtained by varying the pulsed current up and down in a non-monotonic sequence. If the electrical breakdown occurred via the formation of critical pores in the lipid bilayer matrix as described earlier, the growth of such pore defects in the cell membrane did not continue uncontrollably, probably because such pores in the lipid bilayer would be 'pinned' by the presence of proteins in the membrane.

Another possible mechanism that would lead to a sharp breakdown at large transmembrane potentials is via catastrophic electrostriction of the proteins imbedded in the membrane. This can occur as follows. In a protein module the elec-

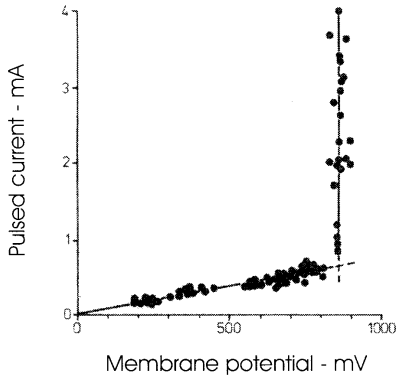

Figure 23. The voltage-current curve for 0.5 mS pulsed currents in the membrane of *Valonia utricularis*. The data points shown were not obtained in order of increasing potential. The electrical breakdown which produced the rapid rise in the current with potential at ~850 mV did not lead to irreversible damage to the cell membrane and the characteristics were very reproducible. This was the first direct demonstration of electrical breakdown in the voltage-current characteristics of cell membranes using pulsed currents (after [32]).

trostriction varies as the square of the field strength and the latter will, of course depend not only on the transmembrane potential but also on the thickness of the protein module. The elastic restoring forces that balance the electrostriction will, ideally, vary only logarithmically. This can clearly lead to a critical point where the electrostrictive compression leads to a catastrophic collapse of the protein in a process by which the field strength continues to grow larger, even at a constant membrane potential difference as the thickness decreases through electrostriction. When this occurs the proteins can no longer be held in place as an integral part of the membrane. The critical potential for this is given occurs when;

$$\frac{\partial P_e}{\partial \delta} = -\frac{\partial P_m}{\partial \delta}$$

The critical breakdown potential for electrostrictive breakdown is then given by [31]:

$$\mathrm{V}_C = \left[\frac{0.3679\mathrm{Y}\mathrm{d}_0^2}{\varepsilon_\mathrm{P}\varepsilon_0}\right]^{\frac{1}{2}} \tag{22}$$

where:
Y is the elastic modulus of the membrane
ε_p is the dielectric constant of the protein
ε_o is the permittivity of free space
d_o is the uncompressed thickness of the module.

If the electrical breakdown occurs through catastrophic electrostriction, one would expect that the critical breakdown potential should vary with temperature

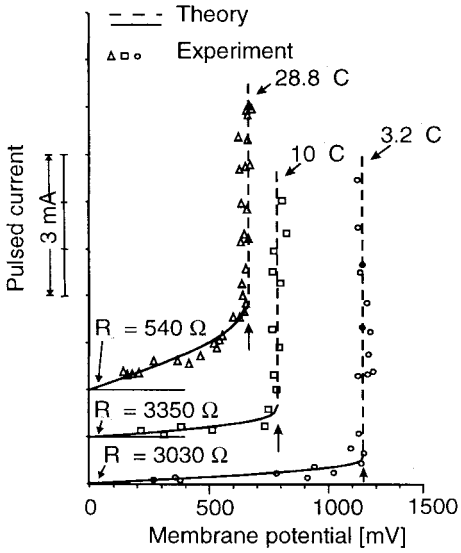

Figure 24. The effect of temperature on the electrical breakdown characteristics of *Valonia utricularis* measured with pulsed currents (0.5 mS pulses). The experimental points on these plots were NOT taken in order of increasing current; they were measured in random order. The theoretical curves were obtained assuming the conduction modules in the membrane undergo electrostriction. Apart from the critical membrane potential for electrical breakdown, which is determined from these plots, the theory has no other adjustable parameters. Data from [31].

as the elastic moduli of materials are generally strongly dependent on temperature. Indeed this is the case. An example [31] of such an effect is shown in Figure 24. Note that the breakdown potential *decreases* with increasing temperature; indicating, on the basis of the electrostriction model, that the elastic modulus decreases with increasing temperature. This would suggest that the elastic properties are determined predominantly by the energetics of deformation of the protein and that the internal configurational entropy is not as important; the proteins do not behave as entropy springs (unlike rubber bands).

PART 4: BIOTECHNOLOGICAL APPLICATIONS

The elucidation of the intriguing electrical properties of cell membranes has not only given us insights into physiological and biochemical functions performed, but have also found interesting and far reaching applications in biotechnology and biomedical science. Below we describe briefly some of these.

4.1 Electroporation

An application of the controlled electrical breakdown of the cell membrane is to produce large, transient, changes in the permeability of the cell membrane. Thus, it is possibile to induce transient permeability to macro-molecules, including strands of DNA. The induction of these transient permeability states by electrical breakdown is known as 'Electroporation'. The technique of electroporation is now a common, and almost essential, tool for genetic engineering and dozens of manufacturers now produce electroporation apparati.

The electrical breakdown phenomenon has also provided an interesting tool for the study of the electro-mechanics of cell membranes. The breakdown potential as well as the electrical characteristics near the breakdown potential differ in different types of cells and vary with the state of the cell and it may prove to be a useful tool for monitoring progressive changes occurring in cells (such as erythrocytes) in certain diseases.

4.2 Cell Dielectrophoresis

When a dielectric particle with a dielectric constant ε_p is suspended in an aqueous solution with a different dielectric constant, ε_s, in a region in which a non-homogeneous electric field is established, the particle will experience a translational force which results from induced electric dipoles. This effect is referred to as 'Dielectrophoresis' [33]. In a uniform electric field there is no net translational force acting on the particle. The direction of the dielectrophoretic force is *independent* of the direction of the field; it is dependent on the field gradient. The dieletrophoretic force for ideal, uniform dielectric particles suspended in a non-conducting medium is also the same for DC or AC electric fields (at least for frequencies below the inverse time constant for electric polarization of the materials).

From a dielectric point of view, living cells can be thought of, in a first approximation, as a particle (cytoplasm) with a dielectric constant ε_c and conductivity σ_c surrounded by a thin membrane with a dielectric constant ε_m and a (very low) conductivity σ_m. The cell is suspended in a solution with a dielectric constant ε_s and conductivity σ_s.

When placed in a uniform, alternating, electric field, the field patterns around such a cell depend strongly on the frequency of the applied field. An example for a typical mammalian cell suspended in a low conductivity aqueous medium ($\sigma_s \sim 1$ mS m^{-1}) is shown in Figure 25 [34]. At low frequencies the electrical currents are carried largely by ionic currents and at these low frequencies, the field is excluded from the cell because the cell membrane is such a poor conductor. At mid frequencies, the membrane capacitance (which has a very large area-specific value because the membrane is very thin) has a relatively low impedance and the field penetrates the cell. Since the cytoplasm is a good electrical conductor (as the ion concentrations in the cytoplasm are relatively large), the field gradients

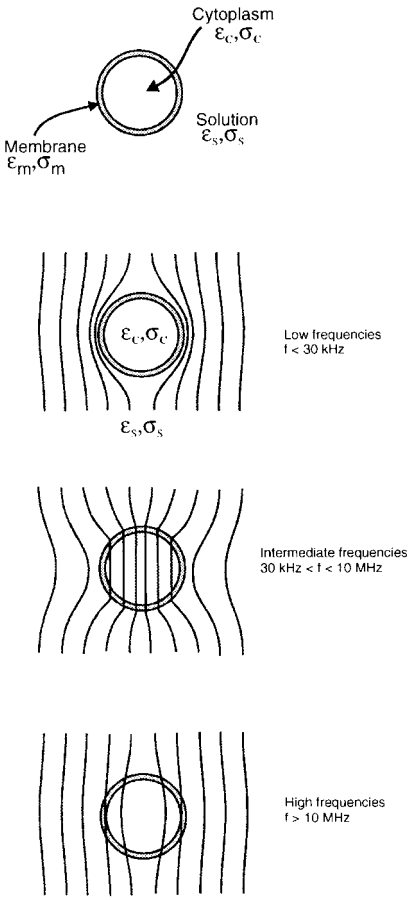

Figure 25. Electric field patterns around a cell suspended in a medium of low conductivity ($\sim$1 mS m^{-1}), for three different frequency regimes. The applied field in the absence of the cell would be uniform. In non-uniform applied electric fields the cell will move through the interaction of the induced dipole with the electric field. At very low and at very high frequencies the dielectrophoresis is negative, that is the cell will move out of the field gradient, whilst at mid frequencies the cell is drawn into the high field region.

in the cytoplasm are very small. The electric currents are then a mixture of ionic currents and displacement currents. At high frequencies, the currents are largely due to displacement currents and the impedance is determined by the dielectric constants of the cytoplasm and the surrounding solution.

Overall, the field patterns around the cell are that of a dielectric particle whose effective dielectric properties vary with frequency; at low frequencies the effective dielectric constant of the 'particle' $\varepsilon_p < \varepsilon_s$, at mid frequencies $\varepsilon_p > \varepsilon_s$ and at very

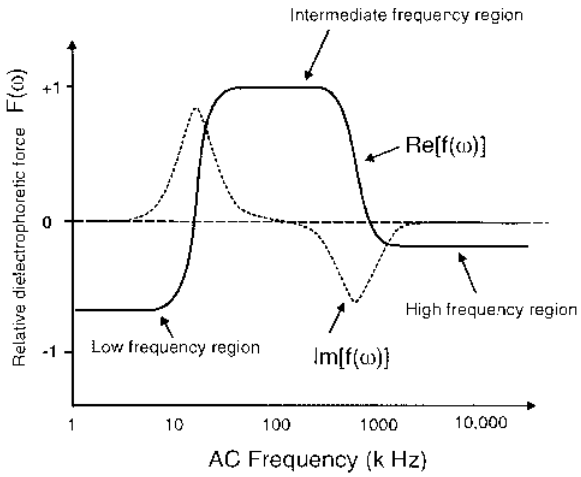

Figure 26. Typical dielectrophoretic force spectra for a cell suspended in an isotonic solution of low ionic strength (conductivity ~1 mS m^{-1}) in an electric field of constant gradient. The force at low frequencies drives the cell out of the high field region (negative dielectrophoresis). At intermediate frequencies the dielectrophoretic force draws the dell into the high field region (positive dielectrophoresis). At very high frequencies the dielectrophoretic force becomes negative again. The cross-over points or reversal frequencies are characteristic of a cell. The dielectrophoretic force function has real and imaginary components. The imaginary component (broken line) shows distinct maxima and minima which are associated with the spinning of the cell in rotating electric fields; the cell spin response shows sharp peaks at these frequencies. The rotational speed of the cell itself typically has maximal values of around 1 Hz (after [34]).

high frequencies $\varepsilon_p < \varepsilon_s$. The dielectric constants are in fact complex and contain a real component, ε, as well as an imaginary component $i\sigma/\omega$.

When a cell is placed in a non-uniform electric field, it will undergo dielectrophoresis and the magnitude and even the sign of the dielectrophoretic force will be dependent on frequency. In general, the cell will be driven out of a high field region at low frequencies and into a high field region at mid frequencies and out of a high field region again (although to a reduced extent) at very high frequencies [34, 35] (see Figure 26.) Measurements of the dielectrophoretic force spectrum for cells, generally are similar to those shown in Figure 26 for an idealised spherical dielectric particle surrounded by a dielectric shell (membrane) and suspended in a third dielectric medium. The detailed spectra for cells are different for different cell types, presumably reflecting differences in the dielectric properties of the membrane etc. as well as features that arise from the more complicated internal structures in living cells. The dielectrophoretic spectra, including the specific cross-over points in the spectra where the dielectrophoretic forces changes sign, can be used to distinguish and selectively manipulate cells.

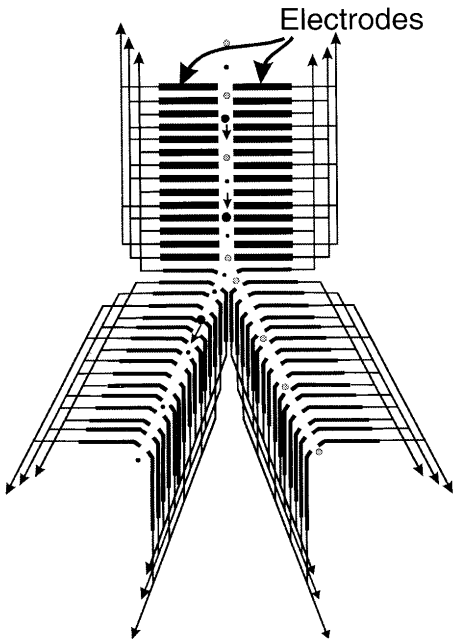

Figure 27. Cell movement using electrode tracks in which cells can be moved by travelling-wave dielectrophoresis. By applying signals of different frequencies to the electrodes in the two branches, it is possible to separate different types of cells by their dielectric properties (after [36]).

4.3 Cell Selection and Trapping

Dielecctrophoresis can be used to move cells either between electrodes or along tracks of electrodes energised by AC signals. This can be achieved by arranging linear sets of electrodes grouped in sets of 4 electrodes, in which the AC applied to the eltrode pairs in each half of the track are 90° out of phase with subsequent pairs. A schematic of the electrode set-up is shown in Figure 27 [36]. As the dielectrophoretic force depends on the AC frequency as well as the properties of the cell, it is possible to separate a mixture of cells using a split track of electrodes energised at different frequencies; see illustration in Figure 27.

It is possible also to trap cells using two sets of electrodes connected to AC signal generators that have AC waveforms 90° out of phase; see Figure 27. The cells in such a system tend to execute spiralling orbits towards the centre. The physics of this cell trap are essentially identical to the systems designed for trapping nuclear particles that were invented by the Nobel-prize winner, Wolfgang Paul.

4.4 Cell Fusion

Controlled electroporation can also be used to cause two cells, brought into close contact, to fuse with each other. Radio frequency electric fields can be utilised to bring the cells together by positive dielectrophoresis or the cells maybe mechanically manipulated into position. Electrical breakdown in the two cell membranes at their point of contact can then be induced via the application of current pulses applied to electrodes in the solution. This technique has now been perfected and has been used to create a variety of plant, animal and human hybrid cells [37]. New cell types of almost any species, or even cross species, can in principle so be created.

References

1. Coster, H.G.L. and Kaplin, I.J.: *Biochim. Biophys. Acta* **330** (1973), 141–146.
2. Overton, E.: *Vjschr. Naturf. Ges. Zurich.* **44** (1899), 88–113.
3. Danielli, H.A. and Davson, J.F.: *J. Cell. Comp. Physiol.* **5** (1935), 495–508.
4. Gorter, E. and Grendel, F.: *J. Exp. Med.* **41** (1925), 439.
5. Fricke, H. and Morse, S.: *J. Gen. Physiol.* **9** (1925), 153–167.
6. Robertson, J.D.: *Biochemical Society Symp.* **3** (1959).
7. Mueller, R., Rudin, D.O., Tien, H.T. and Wescott, W.C.: *Nature* **194** (1962), 979–981.
8. Singer, S.J. and Nicholson, G.L.: *Science* **175** (1972), 720–731.
9. Israelachvilli, J.N., Mitchell, D.J. and Ninham, B.W.: *J. Chem. Soc. Far. Trans. II* **72** (1976), 1525–1568.
10. Bloom, M., Evans, E. and Mouritsen, O.G.: *Quarterly Reviews of Biophysics* **24** (1991), 293–397.
11. Israelachvili, J.N.: *Biochim. Biophys. Acta* **469** (1977), 221–225.
12. Langmuir, I. and Blodgett, K.: *Kolloid-Z.* **73** (1935), 258–263.
13. Israelachvili, J.N., Mitchell, D.J. and Ninham, B.W.: *J. Chemical Soc., Faraday Trans. II* **72** (1976), 1525–1568.
14. Coster, H.G.L. and Simons, R.: *Biochim. Biophys. Acta* **163** (1968), 234–239.
15. Tien, H.T.: *Bilayer Lipid Membranes, Theory and Practice*, Marcel Dekker Inc, New York, 1975.
16. Coster, H.G.L. and Smith, J.R.: *Biochim. Biophys. Acta* **373** (1974), 151–164.
17. Tien, H.T., Dianna, A.L. and Louise, A.: *Nature* **215** (1967), 1199.
18. Fettiplace, R., Andrews, D.M. and Haydon, D.A.: *J. Membrane Biol.* **5** (1971), 277–296.
19. Hanai, T., Haydon, D.A. and Taylor, J., A., H.D. and Taylor, J.L.: *Proc. Roy. Soc. London, Ser A* **281** (1964), 377.
20. Huang, W.T. and Levitt, D.G.: *Biophys. J.* **17** (1977), 111–128.
21. Born, M.: *Z. Phys.* **1** (1920), 45–48.
22. Neumcke, B. and Läuger, P.: *Biophys. J.* **9** (1969), 1160–1170.
23. Coster, H.G.L.: *Aust. J. Phys.* **52** (1999), 117–140.
24. Taupin, C., Dvolaitzky, M. and Sauterey, C.: *Biochemistry* **14** (1975), 4771–4775.
25. Abidor, I.G., Arakelyan, V.B., Chernomordik, L.V., Chizmadzhev, Y., A., Pastushenko, V.F. and Tarasevich, M.R.: *Bioelectrochem. Bioenergetics* **6** (1979), 37–51.
26. Coster, H.G.L.: In: G.M. Eckert (ed.), *Electropharmacology*, CRC Press, Florida, 1990, pp 139–150.
27. Parsigian, V.A.: *Ann. N.Y. Acad. Sci.* **264** (1975), 161.
28. Smith, J.R., Laver, D.R. and Coster, H.G.L.: *Chem. Phys. Lipids* **34** (1984), 227–236.

29. Ashcroft, R.G., Coster, H.G.L. and Smith, J.R.: *Biochim. Biophys. Acta* **643** (1981), 191–204.
30. Karolis, C., Coster, H.G.L., Chilcott, T.C. and Barrow, K.D.: *Biochim. Biophys. Acta* **1368** (1998), 247–255.
31. Coster, H.G.L. and Zimmermann, U.: *J. Membrane Biol.* **22** (1975), 73–90.
32. Coster, H.G.L. and Zimmermann, U.: *Z. Naturforsch.* **30** (1975), 77–79.
33. Pohl, H.A.: *Dielectrophoresis, The Behaviour of Neutral Matter in Non-Uniform Electric Fields*, Cambridge University Press, Cambridge, 1978.
34. Mahaworasilpa, T.L., Coster, H.G.L. and George, E.P.: *Biochim. Biophys. Acta* **1193** (1994), 118–126.
35. Mahaworasilpa, T.L., Coster, H.G.L. and George, E.P.: *Biochim. Biophys. Acta* **1281** (1996), 5–14.
36. Pethig, R. and Markx, G.H.: *Trends Biotechnol.* **32** (1997), 337–343.
37. Coster, H.G.L., Ashcroft, R.G. and Mahaworasilpa, T.L.: PCT/AU92/00473, 1992.
38. Coster, H.G.L.: *Biophys. J.*, **5** (1965), 669–686.